Fidelity of the near-resonant quantum kicked rotor

2011 J. Phys. A: Math. Theor. 44 335101

(http://iopscience.iop.org/1751-8121/44/33/335101)

J. Phys. A: Math. Theor. **44** (2011) 335101 (12pp) doi:10.1088/1751-8113/44/33/335101

Fidelity of the near-resonant quantum kicked rotor

B Probst, R Dubertrand[1] **and S Wimberger**

Institute for Theoretical Physics and Center for Quantum Dynamics, University of Heidelberg, Philosophenweg 19, D-69120 Heidelberg, Germany

E-mail: remy.dubertrand@bristol.ac.uk

Received 14 April 2011, in final form 4 July 2011
Published 27 July 2011
Online at stacks.iop.org/JPhysA/44/335101

Abstract
We present a perturbative result for the temporal evolution of the fidelity of the quantum kicked rotor, i.e. the overlap of the same initial state evolved with two slightly different kicking strengths, for kicking periods close to a principal quantum resonance. Based on a pendulum approximation, we describe the fidelity for rotational orbits in the pseudo-classical phase space of a corresponding classical map. Our results are compared to numerical simulations indicating the range of applicability of our analytical approximation.

PACS numbers: 03.65.Sq, 05.60.Gg, 03.75.Dg, 37.10.Vz

(Some figures in this article are in colour only in the electronic version)

1. Introduction

In classical mechanics, chaos can be defined using the stability of a trajectory. Consider two neighbouring phase-space points, the distance of their orbits in the phase space will grow exponentially in time for a generic chaotic system. Such an approach is bound to fail in a quantum mechanical treatment as the time evolution is unitary and the overlap of two wave packets is constant in time. However, changing a parameter of the Hamiltonian instead of the initial state will lead to an overlap varying in time. This idea was formulated by Peres [1] when he introduced the fidelity, also known as Loschmidt echo [2]. The fidelity is defined as the overlap of an initial state evolved with slightly different Hamiltonians. This quantity has been used to characterize the stability of quantum states [3]. For classically chaotic systems, the fidelity shows some generic behaviour [3].

Here, we study the fidelity in the quasi-integrable regime for which not so many results are established [4–8]. We will do this for one of the best-known examples of classically chaotic system: the kicked rotor (KR) [9, 10]. In order to understand the fingerprints of classical chaos in quantum mechanics, the quantum kicked rotor (QKR) has been and still is a fruitful field of study [11]. It shows several interesting phenomena like quantum resonance [12]

[1] Present address: School of Mathematics, University of Bristol, University Walk, Bristol BS8 1TW, UK.

and dynamical localization [13] both in direct contradiction to the behaviour of the classical system. In the implementation of the QKR near a quantum resonance in the gravity field, Oberthaler *et al* observed quantum accelerator modes [14]. Fishman *et al* were able to describe these theoretically using a pseudo-classical limit. There the detuning of the kicking period to its resonant value plays the role of the Planck constant [15]. Using this treatment, the QKR can be mapped onto a kicked rotor with a renormalized kicking strength. This leads to regular structures and allows the application of semi-classical methods in the pseudo-classical limit although the system might be chaotic in the true semi-classical limit [16].

The KR shows two types of motion in the quasi-integrable regime: oscillations about the stable fixed points and rotating motion. The motion on the classical resonance island surrounding the fixed point leads to revivals of the quantum fidelity. This was shown for the regular QKR by Sankaranarayanan *et al* [5] and for the near resonant QKR by Abb *et al* [6]. Similar results were obtained for another kicked system by Krivolapov *et al* [7]. Rotational and oscillating orbits were also numerically studied in [8]. Our focus in this paper is to treat the rotating modes of the QKR near a quantum resonance. Therefore, we use the pseudo-classical method and apply the pendulum approximation. Section 2 sets the stage by reviewing the pseudo-classical approximation and defining the fidelity which is studied here. In section 3, we give a perturbative treatment of the pendulum and discuss its validity based on a comparison with numerical simulations in section 4. An additional numerical check is shown in section 5.

2. Fidelity for the atom-optical kicked rotor

The story of the experimental investigation of the QKR is quite long [17] and it has been continuing until today (see, e.g., [18–20] and, for fidelity measurements specifically, [21]). In the experimental realizations, atoms are kicked by a periodic potential formed by a standing wave of laser light, i.e. an optical lattice which is flashed on and off periodically in time [17, 22]. Using rescaled dimensionless momentum p, position x, kicking period τ and kicking strength k, see e.g. [15], the Hamiltonian for one kicked atom is

$$H(p, x, t) = \frac{p^2}{2} + k\cos(x)\sum_{n=-\infty}^{\infty}\delta(t - n\tau). \tag{1}$$

The Floquet operator mapping the state right after one kick to the state right after the next kick is, see e.g. [11],

$$\hat{\mathcal{U}} = \mathrm{e}^{-\mathrm{i}k\cos(\hat{X})}\,\mathrm{e}^{-\mathrm{i}\frac{\tau}{2}\hat{P}^2}. \tag{2}$$

The dynamics is obtained by repeated application of this operator. In contrast to the usual kicked rotor, a kicked atom lives along a line. Performing a gauge transformation one can still recover a problem with conserved quasi-momentum, see e.g. [15, 16]. Here, the quasi-momentum corresponds to the fractional part of the momentum $p = n + \beta$, where n is an integer and β is a real variable between 0 and 1. The problem of one atom along a line is mapped onto a problem of a continuous family of rotors. Each of them corresponds to one value of β. That is the reason why we will speak from now on of a β-rotor. In realizations of the kicked rotor with Bose–Einstein condensates, it has been checked that the interactions between atoms in the cloud can be neglected [18, 19]. This brings another justification of our one-particle approach. The wavefunction of a single β-rotor $|\Psi_\beta\rangle$ is obtained from the wavefunction of the kicked atom $|\psi\rangle$ by [15, 16]

$$\langle\theta|\Psi_\beta\rangle = \frac{1}{\sqrt{2\pi}}\sum_{n\in\mathbb{Z}}\langle n + \beta|\psi\rangle\,\mathrm{e}^{\mathrm{i}n\theta}, \tag{3}$$

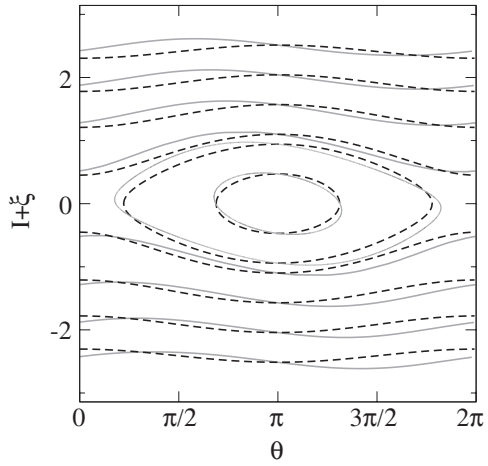

Figure 1. Phase space of the pendulum (black - - - -) and the kicked rotor (grey ——) for $\tilde{k} = |\epsilon|k = 0.08\pi$.

while the Floquet operator for one β-rotor is

$$\hat{\mathcal{U}}_\beta = \mathrm{e}^{-\mathrm{i}k\cos\hat{\theta}}\,\mathrm{e}^{-\mathrm{i}\frac{\tau}{2}(\hat{\mathcal{N}}+\beta)^2}, \tag{4}$$

where $\hat{\mathcal{N}}$ is the angular momentum operator. The operator (4) formally differs from the usual Floquet operator [11] only by the quasi-momentum β.

A principal quantum resonance occurs in the kicked particle when the phase due to the free evolution in (4) vanishes [23]. Each resonance leads to a ballistic motion and a quadratic growth of the energy. This happens at $\tau = 2\pi l$ and for resonant quasi-momenta $\beta_{\mathrm{res}} = 1/2 + q/l$ for integers l and q such that $l \geqslant 1$ and $0 \leqslant q \leqslant l-1$. To simplify the notation, in this paper, we consider the specific resonance with $\tau = 2\pi$ and $\beta_{\mathrm{res}} = 1/2$.

Take now a kicking period slightly detuned from its resonant value $\tau = 2\pi + \epsilon$. Introducing the rescaled momentum $\hat{I} = |\epsilon|\hat{\mathcal{N}}$, we can rewrite the Floquet operator (4) as

$$\hat{\mathcal{U}}_{k,\beta} = \mathrm{e}^{-\frac{\mathrm{i}}{|\epsilon|}\tilde{k}\cos(\hat{\theta})}\,\mathrm{e}^{-\frac{\mathrm{i}}{|\epsilon|}[\mathrm{sgn}(\epsilon)\frac{\hat{I}^2}{2}+\hat{I}(-\pi+\tau\beta)]}. \tag{5}$$

This operator can be identified as the formal quantization of another *fictitious* kicked rotor. The main benefit of this mapping is that the kicking strength of the new problem is $\tilde{k} = |\epsilon|k$ and $|\epsilon|$ plays the role of the Planck constant. We will be interested from now on in the regime $|\epsilon| \to 0$, called the ϵ-semiclassical limit [15], which must not be confused with the *true* semiclassical one of the initial problem. In the ϵ-semiclassical limit, one can derive easily the ϵ-classical map, which is very similar to the celebrated standard map [9]:

$$\begin{aligned} I_{t+1} &= I_t + \tilde{k}\sin(\theta_{t+1}) \\ \theta_{t+1} &= \theta_t + \mathrm{sgn}(\epsilon)I_t - \pi + \tau\beta \mod 2\pi. \end{aligned} \tag{6}$$

We are interested in the dynamics around a stable fixed point of (6). One common approximation is the pendulum approximation [9, 10]:

$$H_{\mathrm{Pen}}(I,\theta) = \frac{(I+\xi)^2}{2} + \tilde{k}\cos\theta, \tag{7}$$

where we have defined $\xi = \mathrm{sgn}(\epsilon)(-\pi + \tau\beta)$. For a given (even large) kicking strength k, one can always choose a small enough ϵ so that we are in the quasi-integrable regime. This makes the phase spaces corresponding to (6) and (7), respectively, very similar, see figure 1.

The main goal of this paper is to check the stability of the quantum dynamics under slight variation of the kicking strength. The fidelity [1, 3] appears as the natural quantity to look at. For one single β-rotor it is defined as

$$F_\beta(k_1, k_2, t) = |\langle\psi_0|\mathcal{U}^{t\ \dagger}_{k_1,\beta}\,\mathcal{U}^t_{k_2,\beta}|\psi_0\rangle|^2. \tag{8}$$

For the initial problem of a kicked atom one needs to consider the fidelity for a sub-ensemble of rotors, which is defined then by [24, 25]

$$F(k_1, k_2, \beta_1, \Delta\beta, t) = \left|\int_{\beta_1}^{\beta_1+\Delta\beta} \frac{\mathrm{d}\beta}{\Delta\beta}\langle\psi_0|\mathcal{U}^{t\ \dagger}_{k_1,\beta}\,\mathcal{U}^t_{k_2,\beta}|\psi_0\rangle\right|^2. \tag{9}$$

If the initial state mainly lives on the stable island, the fidelity shows revivals as explained in [6], see also a similar context in [7]. Here, the study will be devoted to the fidelity (8) in the neighbourhood of such an island. We will approximate (8) by the fidelity of the pendulum (7). The fidelity of the pendulum is obtained by expanding the initial state in the eigenbasis $|\phi_n(k)\rangle$ of the Hamiltonian[2] of equation (7), which depends on β via ξ

$$F_\beta(k_1, k_2, t) = \left|\sum_{n,m}\langle\Psi_\beta(t=0)|\phi_n(k_2)\rangle\langle\phi_n(k_2)|\phi_m(k_1)\rangle\langle\phi_m(k_1)|\Psi_\beta(t=0)\rangle\,\mathrm{e}^{\mathrm{i}\frac{t}{|\epsilon|}(E_n^{k_2}-E_m^{k_1})}\right|^2. \tag{10}$$

Throughout the paper we focus on the quantum problem associated with (5) so that $|\epsilon|$ is always our Planck constant. This is the reason why we will call the ϵ-semiclassical regime simply the semiclassical regime.

3. Perturbative treatment of the pendulum

We are interested in the quantum pendulum following the approximation (7). It is well known that this system is quantum mechanically integrable [26]. Following (10), we want to obtain simple explicit formulae for the eigenenergies E_n^k and the eigenfunctions $|\phi_n(k)\rangle$ of the Hamiltonian when $|\epsilon|$ is going to 0. We will follow standard perturbation theory. The only unusual thing is that the potential is proportional to the effective Planck constant so that it vanishes at the classical limit $|\epsilon| = 0$.

Our unperturbed system is a free particle along a ring with eigenenergy and eigenfunction ($m \in \mathbb{Z}$):

$$E_m = \frac{(m|\epsilon| + \xi)^2}{2} = \frac{\xi^2}{2} + \xi m|\epsilon| + \mathcal{O}(|\epsilon|^2), \tag{11}$$

$$\langle\theta|\phi_m\rangle = \frac{\mathrm{e}^{\mathrm{i}m\theta}}{\sqrt{2\pi}}. \tag{12}$$

For $\tilde{k} > 0$, the Schrödinger equation for the stationary states becomes

$$\frac{1}{2}\left(-\mathrm{i}|\epsilon|\frac{\partial}{\partial\theta} + \xi\right)^2\Psi + \tilde{k}\cos\theta\Psi = E\Psi. \tag{13}$$

Performing the gauge transformation $\Psi = \exp(-\mathrm{i}\xi\theta/|\epsilon|)\psi$ and setting $\psi(\theta) = f(z = \theta/2)$, equation (13) becomes

$$\frac{\mathrm{d}^2 f}{\mathrm{d}z^2} + \left(\frac{8E}{|\epsilon|^2} - 2\frac{4\tilde{k}}{|\epsilon|^2}\cos(2z)\right)f(z) = 0, \tag{14}$$

[2] We emphasize the dependence of the eigenstates on k as it is the perturbation parameter in the fidelity.

which is the standard form of Mathieu equation, see e.g. 16.2.1 p 97 in [27]. For our purpose it is easier to look for a solution of (14) as the following series:

$$f(z) = \sum_{n\in\mathbb{Z}} c_n \, \mathrm{e}^{(\mu+2\mathrm{i}n)z}. \tag{15}$$

As we require the 'true' wavefunction $\Psi(\theta)$ to be univalued, one can easily see that we need

$$\mu = \frac{2\mathrm{i}\xi}{|\epsilon|}. \tag{16}$$

The eigenenergies of (13) are given by characteristic values of Mathieu functions, which do not lead to simple explicit formulae. A semiclassical approach is rather used to write an expansion of the eigenenergies. The details are found in the appendix. The results are, assuming $\tilde{k} = k|\epsilon|$ and noting $\xi_0 = \mathrm{sgn}(\epsilon)\pi(2\beta - 1)$,

$$\begin{aligned} E_m^k \simeq \frac{\xi_0^2}{2} + \xi_0(m+\beta)|\epsilon| + \left(\frac{(m+\beta)^2}{2} + \frac{k^2}{4\xi_0^2}\right)|\epsilon|^2 - \frac{(m+\beta)k^2}{2\xi_0^3}|\epsilon|^3 \\ + \left(\frac{3}{4}\frac{(m+\beta)^2k^2}{\xi_0^4} + \frac{5}{64}\frac{k^4}{\xi_0^6}\right)|\epsilon|^4. \end{aligned} \tag{17}$$

In (15) the coefficients c_n are the solutions of the following recurrence relation:

$$[2E - (n|\epsilon| + \xi)^2]c_n = \tilde{k}(c_{n-1} + c_{n+1}). \tag{18}$$

If we assume now that we start from an unperturbed state (12) with the energy (11), (18) can be rewritten as

$$2\frac{(n-m)\xi_0}{-k}c_n^{(m)} = c_{n-1}^{(m)} + c_{n+1}^{(m)}, \tag{19}$$

which gives the solution $c_n^{(m)} = J_{n-m}(-k/\xi_0)$, where $J_n(x)$ stands for the Bessel function of integer order n. The perturbed eigenfunctions are then

$$\langle\theta|\phi_m(k)\rangle = \sum_{n\in\mathbb{Z}} J_{n-m}\left(\frac{-k}{\xi_0}\right)\mathrm{e}^{\mathrm{i}n\theta} = \mathrm{e}^{\mathrm{i}m\theta - \mathrm{i}k\sin(\theta)/\xi_0}, \tag{20}$$

where we have used in the second equality the following identity for the Bessel functions, see e.g. 7.2.4(26) p 7 in [28]:

$$\sum_{n\in\mathbb{Z}} J_n(x)\mathrm{e}^{\mathrm{i}n\theta} = \mathrm{e}^{\mathrm{i}x\sin\theta}. \tag{21}$$

The great benefit from (20) is that we can directly compute the overlap coefficient for the fidelity (10). We assume that the initial state is a plane wave with momentum n_0: $\langle n|\Psi_\beta(t=0)\rangle = \delta_{n,n_0}$, where $\delta_{n,k}$ is the Kronecker symbol. Then

$$\langle\phi_m(k)|\Psi_\beta(t=0)\rangle = \sum_{n\in\mathbb{Z}}\langle\phi_m(k)|n\rangle\langle n|\psi_\beta(t=0)\rangle = J_{n_0-m}\left(\frac{-k}{\xi_0}\right), \tag{22}$$

$$\begin{aligned} \langle\phi_m(k_1)|\phi_n(k_2)\rangle &= \sum_{p\in\mathbb{Z}}\langle\phi_m(k_1)|p\rangle\langle p|\phi_n(k_2)\rangle \\ &= J_{m-n}\left(-\frac{k_2-k_1}{\xi_0}\right). \end{aligned} \tag{23}$$

Finally, our simple perturbative approach lets us write an explicit formula for the fidelity, reminding $\xi_0 = \mathrm{sgn}(\epsilon)\pi(2\beta - 1)$:

$$F_\beta(k_1,k_2,t) = \left|\sum_{n,m\in\mathbb{Z}} J_{m-n}\left(\frac{k_1-k_2}{\xi_0}\right)J_{n_0-m}\left(\frac{-k_1}{\xi_0}\right)J_{n_0-n}\left(\frac{-k_2}{\xi_0}\right)\mathrm{e}^{\mathrm{i}\frac{t}{|\epsilon|}(E_n^{k_2}-E_m^{k_1})}\right|^2, \tag{24}$$

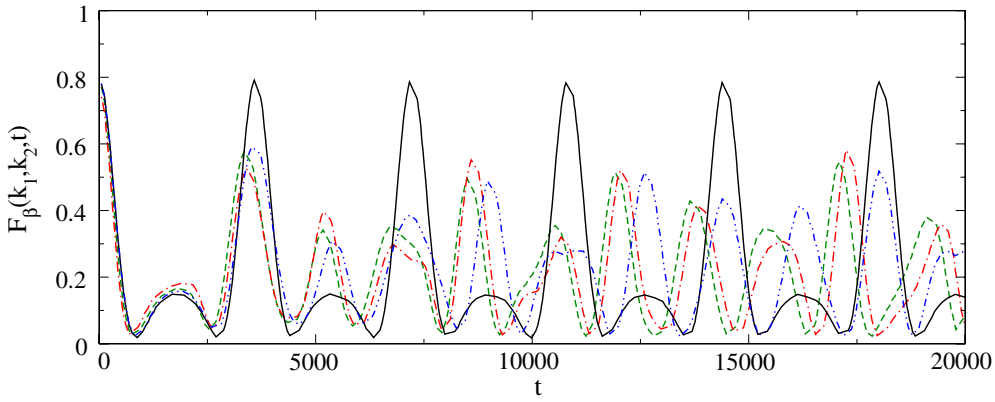

Figure 2. Fidelity using the pendulum (green - - - -), the perturbative result with the third (black ——) and fourth (blue — · · —) order in $|\epsilon|$ in the energy and the original QKR (red — · —). $\beta = 0.3$, $\epsilon = 0.05$, $k_1 = 0.6\pi$ and $k_2 = 0.8\pi$. The data are averaged over 100 kicks in order to cancel fast oscillations.

where $E_m^{k_1}$ and $E_n^{k_2}$ are given by (17). Formula (24) is the main result of this paper. In the following section, we will estimate numerically the range of validity and the accuracy of (24) to describe the QKR. In figure 2, we can already see that the more orders we take for the energy, the more accurate we get.

4. Numerical comparison of the approaches

The perturbative approach, cf equation (24), will now be checked numerically in this section. As single rotors and ensembles show qualitatively different behaviour, we treat these cases separately.

Before showing the main results, we discuss the intrinsic limitations of our approach. The phase space of the pendulum is the cylinder whereas the phase space of the KR can be mapped onto a torus. The pendulum approximation is, therefore, only valid in one phase-space cell of the KR. Due to this mismatch we expect the approximation to fail at the border of a cell.

In the derivation of the perturbative result, we explicitly focused on the rotating regime, which means that our results have to fail in the description of states on the island. The half-width of the island in the pendulum approximation is given by $\Delta I = 2\sqrt{k|\epsilon|}$ [10], which becomes in units of the quasi-momentum

$$\Delta\beta_c^{\text{th}} = \frac{\Delta I}{\tau} \approx \sqrt{\frac{|\epsilon|k}{\pi^2}}. \tag{25}$$

When the distance from β to its resonant value (centred at the island) is less than $\Delta\beta_c$, we expect to observe the revivals in the fidelity as described in [6].

4.1. Single rotors

The most important goal of the discussion of single rotors is to get an intuition for the quality of the pendulum approximation. We can discuss this step only for single rotors as the calculation of the pendulum fidelity is numerically very challenging. Averaging the fidelity over 100 kicks allows us to identify maxima in the two cases and to read the amplitude and the period (cf, for

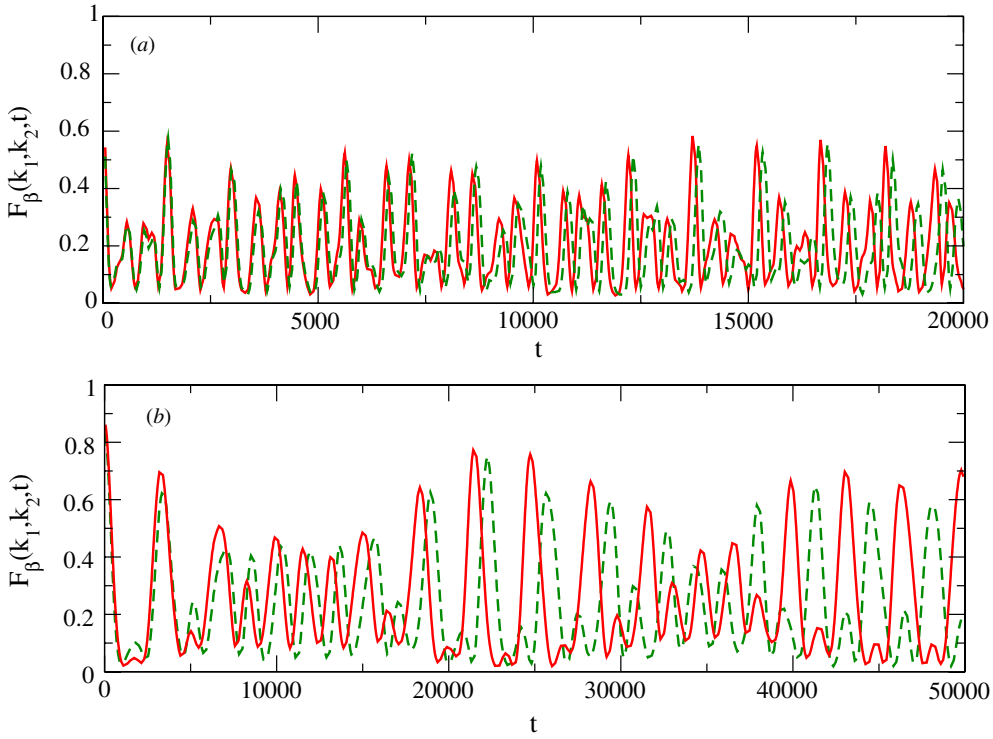

Figure 3. Fidelity for the QKR (red ——) and the pendulum (green - - - -) for $\epsilon = 0.075$, $k_1 = 0.6\pi$ and $k_2 = 0.8\pi$. (*a*) $\beta = 0.3216$, (*b*) $\beta = 0.2412$. The data are averaged over 100 kicks in order to get rid of the fast oscillations.

instance, figure 3). Plotting the relative deviation of the period of the maxima, one observes that this relative error is nearly independent of the choice of the maximum. As a measure of deviation of the amplitude, we compared a limited number of maxima, whilst these maxima should be visible both in the QKR and the pendulum data. We decide to take the maximal deviation within the first ten maxima.

When requiring an accuracy of 10%, we can give as a boundary of validity $\beta \gtrsim 0.2$. In the case of the amplitude, the criterion is not as clear. Taking also the deviation in the amplitude into account, we concluded that $\beta \gtrsim 0.3$ following this criterion.

4.2. Ensembles

In order to build ensembles we need to evaluate the integral in (9). This integral is approximated by a Riemann sum with N_β values of β uniformly distributed in $[\beta_1, \beta_1 + \Delta\beta]$. It has been checked that N_β should be of the order of a few thousand to get a reasonably good approximation for the integral in (9).

For the boundary of the phase-space cell the same criterion as used for single rotors is applied. In figure 4 (*a*), a few ensembles are shown. For the measure of correspondence, we compare the widths of the first few pseudo-oscillations and also demand a deviation of less than 10% here. The onset of the island behaviour near to a resonance leads to small peaks in the fidelity as described in [6]. Therefore, the occurrence of these peaks defines the critical

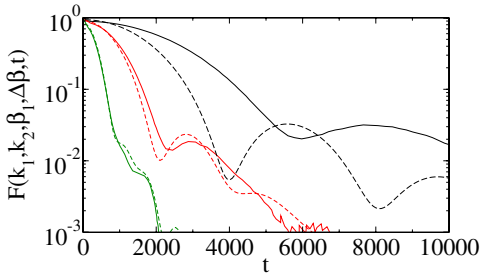

Figure 4. Comparison between the fidelity for the perturbative approach (dashed line) and the QKR (solid line), $\epsilon = 0.05$, $k_1 = 0.6\pi$, $k_2 = 0.8\pi$, $\Delta\beta = 0.06$, $\beta_1 = 0.06$ (black, right), $\beta_1 = 0.14$ (red, middle), $\beta_1 = 0.22$ (green, left).

Table 1. Range of validity of the pendulum approximation. For simplicity we defined $\beta_2 = \Delta\beta + \beta_1$.

ϵ	Range for ensemble	Theoretical upper bound
0.1	0.10–$0.16 < \beta_1, \beta_2 < 0.36$–$0.37$	0.34
0.05	0.12–$0.16 < \beta_1, \beta_2 < 0.39$–$0.41$	0.39
0.01	0.12–$0.16 < \beta_1, \beta_2 < 0.45$–$0.47$	0.45

value near the resonance island. The intervals for several ϵ are summarized in table 1. The upper bound is described quite well by the estimate due to the pendulum approximation (25) and only fails for the largest ϵ presented, i.e. far from the semiclassical regime.

5. Scaling of ensembles

In this section, we perform additional numerical analysis over a larger range of parameters. This will confirm the range of validity of our perturbative approach.

The ensembles in figure 5(*a*) show a similar fidelity as a function of time except for a shift along the time axis. This suggests a rescaling of the time. First choose a reference value of β, say β_{ref}. Then, we claim that we can map the fidelity for *another* β_1 on top of the reference value only by rescaling the time. This can be more formally written in the following way (β_{ref} is chosen *a priori*):

$$F(k_1, k_2, \beta_1, \Delta\beta, t) \approx F(k_1, k_2, \beta_{\mathrm{ref}}, \Delta\beta, \alpha(\beta_1)^{-1}\, t). \tag{26}$$

The fidelity is scaled such that a box surrounding the mean decay can be kept as narrow as possible. An example where the curves in figure 5(*a*) have been rescaled is presented in figure 5(*b*). One may note that formula (26) comes from heuristic and numerical observations. It is believed to work as long as the pendulum approximation does for the kicked rotor. The latter approximation cannot be controlled in a simple way [9]. That is the reason why we will only give here numerical bounds for the validity of (26).

This scaling procedure was done for several β_1, $\Delta\beta$, ϵ and k_1, whereas k_2 was kept the same. The procedure was repeated for another reference β_{ref}. We expect the curves corresponding to different reference values to be parallel, i.e. a different choice of β_{ref} just leads to a constant offset. The resulting plots are presented in figure 6. We can see that the scaling factor has no strong dependence on any of the parameters shown.

The same scaling procedure has also been performed for the perturbative data computed from (24). In figure 7, we show the comparison between scaling factors of the perturbative

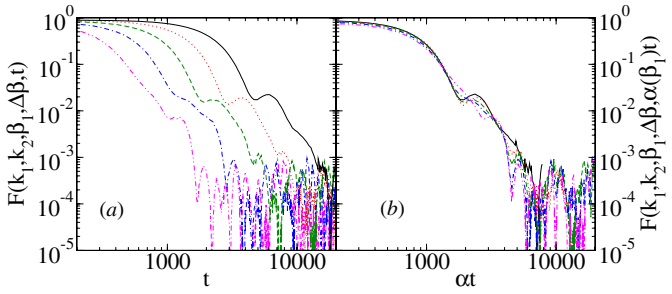

Figure 5. Fidelity of a few ensembles of β-rotors with $\epsilon = 0.05$, $\Delta\beta = 0.06$, $k_1 = 0.6\pi$, $k_2 = 0.8\pi$, $\beta_1 = 0.08$ (black ——), $\beta_1 = 0.12$ (red $\cdots\cdots$), $\beta_1 = 0.16$ (green - - - -), $\beta_1 = 0.2$ (blue — · —) and $\beta_1 = 0.24$ (magenta — · · —). In (a) the original data and in (b) the rescaled data are shown. The scaling factors are according to figure 6.

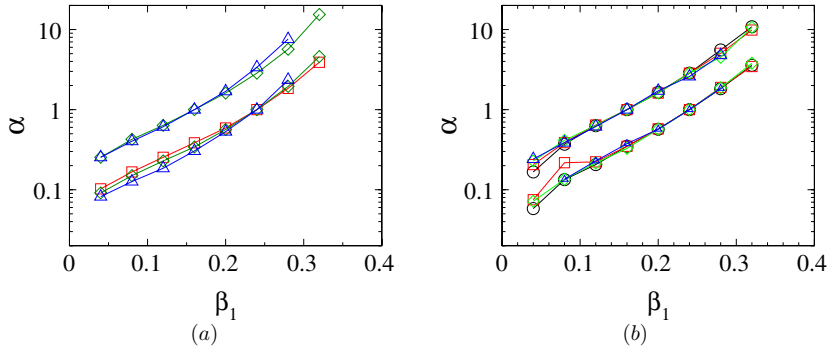

Figure 6. Scaling factors for several parameters. The scaling is done for two references $\beta_{\mathrm{ref}} = 0.16$ (upper curves) and $\beta_{\mathrm{ref}} = 0.24$ (lower curves). $k_2 = 0.8\pi$, $\Delta\beta = 0.03$ (black circles), $\Delta\beta = 0.06$ (red squares), $\Delta\beta = 0.09$ (green diamonds), $\Delta\beta = 0.12$ (blue triangles). (a) $\epsilon = 0.005$, $\Delta k = 0.2\pi$ and (b) $\epsilon = 0.05$, $\Delta k = 0.1\pi$.

result and the QKR for one set of parameters. We observe a reasonable agreement. Below $\beta_1 \approx 0.12$, there is a systematical deviation between equation (24) and the QKR data. This corresponds to the border of the phase-space cell where we already expect the pendulum approach to fail. One may conclude that the rescaling procedure is valid as long as the pendulum approximation holds. More precisely in our case the range of validity is given by the numerical bounds stated above in section 4.2.

6. Summary and outlook

We have for the first time studied analytically the quantum fidelity of initial conditions corresponding to rotational orbits in the underlying pseudo-classical model. Using the pendulum approximation for these orbits, we arrive at our main analytical result summarized in equation (24). Although we use a formally somewhat inconsistent expansion in the perturbation parameter ϵ, we see that our approximation is rather good when including higher orders in the dynamical phases, even if just the lowest order in the amplitude of the wavefunctions is considered. We give clear ranges of applicability of our approximation

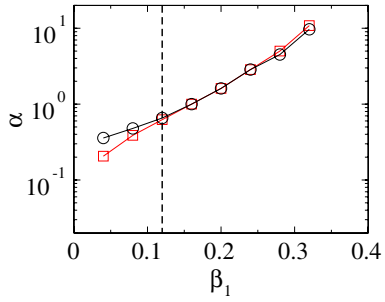

Figure 7. Scaling factors for the perturbative result (black circles) and QKR data (red squares), for $\epsilon = 0.05$, $k_1 = 0.6\pi$, $k_2 = 0.8\pi$, $\beta_{\text{ref}} = 0.16$ and $\Delta\beta = 0.06$. The dashed line is the border of correspondence between the QKR and the perturbative result given in table 1.

which were tested against numerical simulations of the original QKR system. Within these ranges a scaling hypothesis for the temporal decay of the fidelity is found which is fulfilled by the original model as well as our perturbative results. It would be interesting to set this scaling hypothesis onto firm ground by deriving it from first principles for the rotational pseudo-classical orbits investigated here. This task is left for future investigations.

Acknowledgments

It is our great pleasure to thank Italo Guarneri for illuminating discussions at the early stage of this work. This work was supported by the DFG through FOR760, the Helmholtz Alliance Program of the Helmholtz Association (contract HA-216 Extremes of Density and Temperature: Cosmic Matter in the Laboratory), and within the framework of the Excellence Initiative through the Heidelberg Graduate School of Fundamental Physics (grant number GSC 129/1), the Frontier Innovation Fund and the Global Networks Mobility Measures.

Appendix. Perturbative expansion of the pendulum energy levels

We are interested in the quantum energy levels of the pendulum Hamiltonian (7). It is worth recalling that $\tilde{k} = k|\epsilon|$, where $|\epsilon|$ is our effective Planck constant. We are interested in the regime of small $|\epsilon|$. Our procedure is the following: assume first that $|\epsilon|$ is a fixed small quantity. Then write perturbative expansions in $\tilde{k}$, which are valid whenever $\tilde{k} = \mathcal{O}(|\epsilon|)$. Finally, we will write more explicitly $\tilde{k} = k|\epsilon|$ to derive ϵ-semiclassical results.

The classical action for the Hamiltonian (7) along a trajectory from θ_i to θ at a fixed energy E is

$$S(\theta, \theta_i) = \int_{\theta_i}^{\theta} \sqrt{2(E - \tilde{k}\cos\varphi)}\,\mathrm{d}\varphi - \xi(\theta - \theta_i), \tag{A.1}$$

where $\xi = \mathrm{sgn}(\epsilon)(-\pi + \tau\beta) = \xi_0 + |\epsilon|\beta$. The energy level can be well described using a WKB-like approach in the regime $|\epsilon| \to 0$ by

$$\int_0^{2\pi} \sqrt{2\left(E_m^k - \tilde{k}\cos\varphi\right)}\,\mathrm{d}\varphi - 2\xi\pi = 2\pi m|\epsilon|. \tag{A.2}$$

Here, the Maslov index is 0 as the particle lives on a ring, hence never meets any boundary. The quantization condition (A.2) with integers m can be rewritten in a more efficient way as

$$4\sqrt{2\left(E_m^k - \tilde{k}\right)}\,\mathbb{E}\left(\mathrm{i}\sqrt{\frac{2\tilde{k}}{E_m^k - \tilde{k}}}\right) = 2\pi\left[(m+\beta)|\epsilon| + \xi_0\right], \tag{A.3}$$

where $\mathbb{E}(\kappa)$ is the Legendre complete elliptic integral:

$$\mathbb{E}(\kappa) = \int_0^{\pi/2} \sqrt{1 - \kappa^2 \sin(t)^2}\,\mathrm{d}t. \tag{A.4}$$

Equation (A.3) is the starting point of our perturbation expansion. We assume from now onwards that $\xi \neq 0$. For the left-hand side of (A.3), the Taylor expansion of $\mathbb{E}(\kappa)$ is used, see e.g. 8.114 (1) p 853 in [29]:

$$\mathbb{E}(\kappa) = \frac{\pi}{2}\left[1 - \frac{\kappa^2}{4} - \frac{3\kappa^4}{64} - \frac{5\kappa^6}{256} - \frac{175\kappa^8}{16\,384} + \mathcal{O}(\kappa^{10})\right]. \tag{A.5}$$

One obtains

$$\mathbb{E}\left(\mathrm{i}\sqrt{\frac{2\tilde{k}}{E_m^k - \tilde{k}}}\right) = \frac{\pi}{2}\left[1 + \frac{\tilde{k}}{2E_m^k} + \frac{5\tilde{k}^2}{16E_m^{k\,2}} + \frac{9\tilde{k}^3}{32E_m^{k\,3}} + \frac{241\tilde{k}^4}{1024E_m^{k\,4}} + \mathcal{O}\left(\frac{\tilde{k}^5}{E_m^{k\,5}}\right)\right]. \tag{A.6}$$

The eigenenergy E_m^k is assumed to have the following form:

$$E_m^k = \frac{\xi_0^2}{2} + \xi_0(m+\beta)|\epsilon| + \alpha_2\epsilon^2 + \alpha_3|\epsilon|^3 + \alpha_4\epsilon^4. \tag{A.7}$$

Identifying both parts of (A.3) using (A.6) leads to the following results:

$$\alpha_2 = \frac{(m+\beta)^2}{2} + \frac{k^2}{4\xi_0^2} \tag{A.8}$$

$$\alpha_3 = -\frac{(m+\beta)k^2}{2\xi_0^3} \tag{A.9}$$

$$\alpha_4 = \frac{3}{4}\frac{(m+\beta)^2k^2}{\xi_0^4} + \frac{5}{64}\frac{k^4}{\xi_0^6}. \tag{A.10}$$

Inserting (A.8), (A.9) and (A.10) into (A.7) gives (17).

References

[1] Peres A 1984 *Phys. Rev.* A **30** 1610–5
[2] Jalabert R A and Pastawski H M 2001 *Phys. Rev. Lett.* **86** 2490–3
[3] Gorin T, Prosen T, Seligman T H and Znidaric M 2006 *Phys. Rep.* **435** 33–156
Jacquod P and Petitjean C 2009 *Adv. Phys.* **58** 67–196
[4] Benenti G, Casati G and Veble G 2003 *Phys. Rev.* E **68** 036212
[5] Sankaranarayanan R and Lakshminarayan A 2003 *Phys. Rev.* E **68** 036216
[6] Abb M, Guarneri I and Wimberger S 2009 *Phys. Rev.* E **80** 035206
[7] Krivolapov Y, Fishman S, Ott E and Antonsen T M 2011 *Phys. Rev.* E **83** 016204
[8] Weinstein Y S and Hellberg C S 2005 *Phys. Rev.* E **71** 016209
[9] Chirikov B V 1979 *Phys. Rep.* **52** 263–379
[10] Lichtenberg A J and Lieberman M A 1992 *Regular and Chaotic Dynamics* (*Applied Mathematical Sciences* vol 38) 2nd edn (New York: Springer)
[11] Izrailev F M 1990 *Phys. Rep.* **196** 299–392
[12] Izrailev F M and Shepelyanskii D L 1979 *Sov. Phys.—Dokl.* **24** 996
Izrailev F M and Shepelyanskii D L 1980 *Theor. Math. Phys.* **43** 553–61

[13] Fishman S, Grempel D R and Prange R E 1982 *Phys. Rev. Lett.* **49** 509–12
[14] Oberthaler M K, Godun R M, d'Arcy M B, Summy G S and Burnett K 1999 *Phys. Rev. Lett.* **83** 4447–51
[15] Fishman S, Guarneri I and Rebuzzini L 2003 *J. Stat. Phys.* **110** 911–43
[16] Wimberger S, Guarneri I and Fishman S 2003 *Nonlinearity* **16** 1381–420
[17] Moore F L, Robinson J C, Bharucha C F, Sundaram B and Raizen M G 1995 *Phys. Rev. Lett.* **75** 4598–601
[18] Wimberger S, Mannella R, Morsch O and Arimondo E 2005 *Phys. Rev. Lett.* **94** 130404
Rebuzzini L, Artuso R, Fishman S and Guarneri I 2007 *Phys. Rev.* A **76** 031603
[19] Ryu C, Andersen M F, Vaziri A, d'Arcy M B, Grossman J M, Helmerson K and Phillips W D 2006 *Phys. Rev. Lett.* **96** 160403
Talukdar I, Shrestha R and Summy G S 2010 *Phys. Rev. Lett.* **105** 054103
[20] d'Arcy M B, Godun R M, Oberthaler M K, Cassettari D and Summy G S 2001 *Phys. Rev. Lett.* **87** 074102
d'Arcy M B, Godun R M, Summy G S, Guarneri I, Wimberger S, Fishman S and Buchleitner A 2004 *Phys. Rev.* E **69** 027201
Wimberger S, Sadgrove M, Parkins S and Leonhardt R 2005 *Phys. Rev.* A **71** 053404
Kanem J F, Maneshi S, Partlow M, Spanner M and Steinberg A M 2007 *Phys. Rev. Lett.* **98** 083004
Lemarié G, Lignier H, Delande D, Szriftgiser P and Garreau J C 2010 *Phys. Rev. Lett.* **105** 090601
[21] Schlunk S, d'Arcy M B, Gardiner S A and Summy G S 2003 *Phys. Rev. Lett.* **90** 054101
Wu S, Tonyushkin A and Prentiss M G 2009 *Phys. Rev. Lett.* **103** 034101
[22] Graham R, Schlautmann M and Zoller P 1992 *Phys. Rev.* A **45** R19–22
[23] Izrailev F M 1986 *Phys. Rev. Lett.* **56** 541–4
[24] Buchleitner A and Wimberger S 2006 *J. Phys. B: At. Mol. Opt. Phys.* **39** L145–51
[25] Wimberger S 2004 *PhD Thesis* Ludwig-Maximilians-Universität Munich/Università degli Studi dell'Insubria (http://edoc.ub.uni-muenchen.de/archive/00001687)
[26] Condon E U 1928 *Phys. Rev.* **31** 891–4
[27] Erdelyi A *et al* 1953 *Higher Transcendental Functions* vol 3 (New York: McGraw-Hill)
[28] Erdelyi A *et al* 1953 *Higher Transcendental Functions* vol 2 (New York: McGraw-Hill)
[29] Gradsteyn I S and Ryzhik I M 2000 *Table of Integrals, Series and Products* 6th edn (San Diego: Academic)